Supplementary Information for

Inhibition of p300 impairs Foxp3$^+$ T-regulatory cell function and promotes anti-tumor immunity

Yujie Liu[1]†, Liqing Wang[1]†, Jarrod Predina[2], Rongxiang Han[1], Ulf H. Beier[3], Liang-Chuan S. Wang[4], Veena Kapoor[4], Tricia R. Bhatti[1], Tatiana Akimova[1], Sunil Singhal[2], Paul K. Brindle[5], Philip A. Cole[6], Steven M. Albelda[4] & Wayne W. Hancock[1]*

[1]Division of Transplant Immunology, Department of Pathology and Laboratory Medicine, Children's Hospital of Philadelphia and Perelman School of Medicine at the University of Pennsylvania, Philadelphia, PA, USA. [2]Department of Surgery, Perelman School of Medicine at the University of Pennsylvania, Philadelphia, PA, USA. [3]Division of Nephrology, Department of Pediatrics, Children's Hospital of Philadelphia and Perelman School of Medicine at the University of Pennsylvania, Philadelphia, PA, USA. [4]Pulmonary, Allergy & Critical Care Division, Perelman School of Medicine at the University of Pennsylvania, Philadelphia, PA, USA. [5]Department of Biochemistry, St. Jude Children's Research Hospital, Memphis, TN, USA. [6]Department of Pharmacology and Molecular Sciences, Johns Hopkins University School of Medicine, Baltimore, MD, USA.

*Correspondence: Dr. Wayne W. Hancock, Division of Transplant Immunology, Department of Pathology and Laboratory Medicine, Children's Hospital of Philadelphia, 3615 Civic Ctr. Blvd., Philadelphia PA 19104; Telephone: (215) 590-8709, Fax: (215) 590-7384, E-mail: whancock@mail.med.upenn.edu

†These authors contributed equally to this work.

Supplementary Figure 1: Conditional deletion of *Ep300* in T_{reg} cells

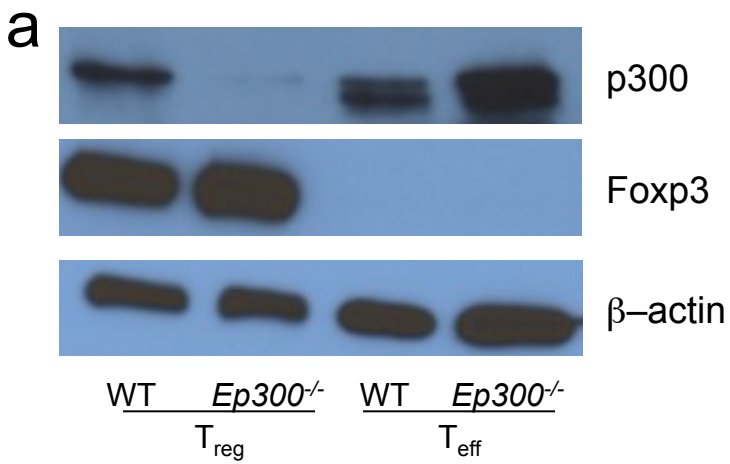

Fig. S1a: Conditional deletion of *Ep300* in T_{reg} cells did not affect Foxp3 expression. Western blotting assessing p300 and Foxp3 expression in T_{reg} or T_{eff} cells from WT and *Ep300*$^{-/-}$ mice. β–actin was used as a loading control.

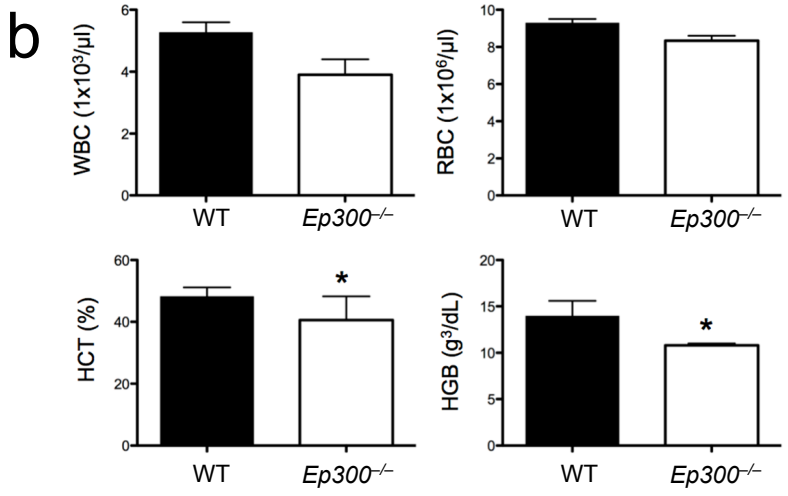

Fig. S1b: Deletion of *Ep300* in T_{regs} was associated with mildly decreased hematocrit (HCT) and hemoglobin (HGB) levels. Data are from 4 mice/group at 10 weeks of age; *p<0.05 vs. control mice.

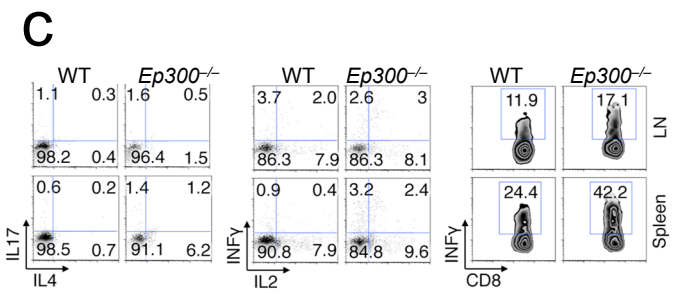

Fig. S1c: T-cells from *Ep300*$^{-/-}$ mice had increased production of proinflammatory cytokines. Cells from lymph node or spleen were stimulated with PMA and ionomycin in the presence of GolgiStop for 5 h. The first two panels (from left to right): cells were gated on CD4^{+} T cells. Numbers in quadrants indicate the percentage of cell population, and data are representative of 4 mice/ group at 10-14 weeks of age.

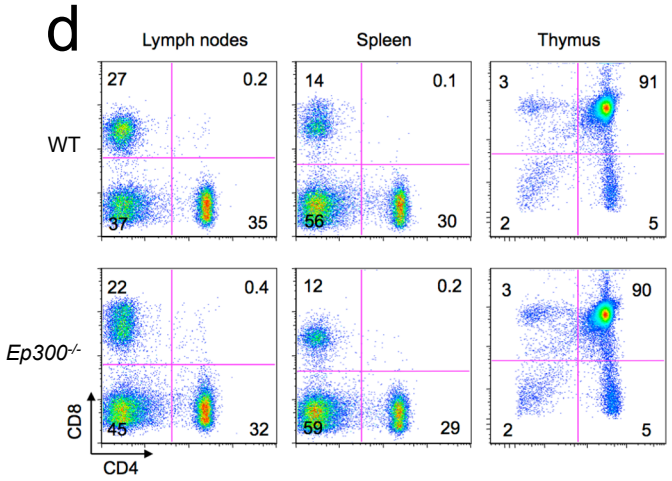

Fig. S1d: Deletion of *Ep300* in T_{regs} did not affect CD4 or CD8 proportions in lymph nodes, spleens or thymii. Numbers in quadrants indicate the percentage of cell population, and data are representative of 4 mice/group at 10 weeks of age.

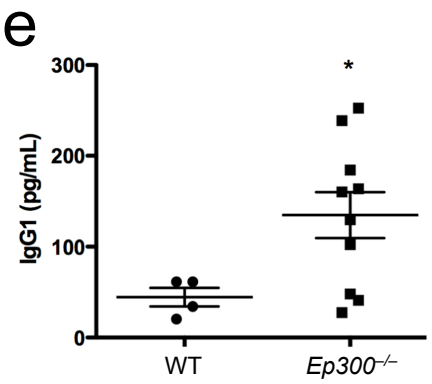

Fig. S1e: Deletion of *Ep300* in T_{regs} led to increased serum IgG1 levels (each symbol indicates the result of an individual mouse, 10 weeks of age, *p<0.05).

Supplementary Figure 2: Microarray analysis of *Ep300*$^{-/-}$ vs. WT T_{regs}

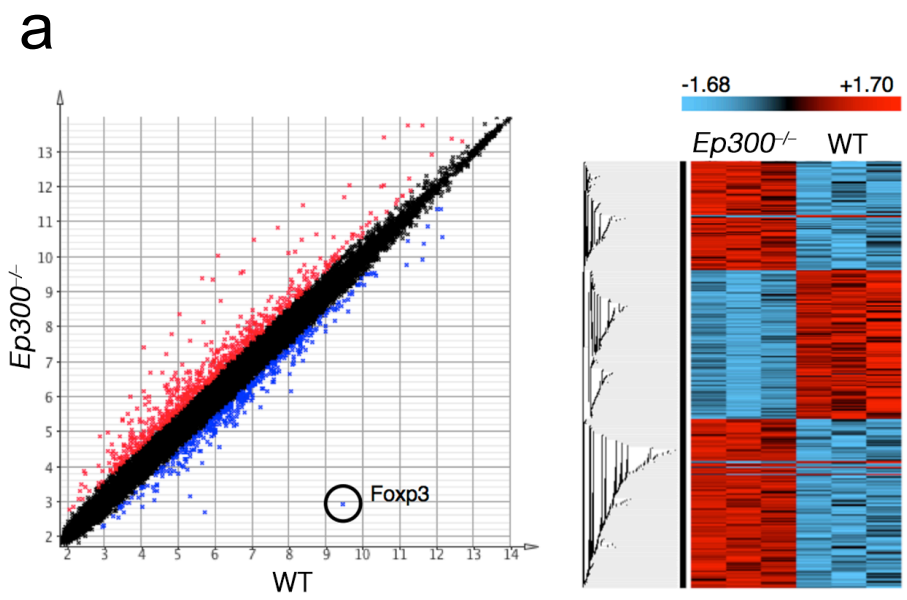

Fig. S2a: Microarray analysis of *Ep300*$^{-/-}$ vs. WT T_{regs}. Left panel shows scatterplot of expression matrix. Probes with 1.5 fold differential expression (log_2 0.5849) are color coded in RED (increased) or BLUE (decreased expression in p300-/-Tregs). Decreased Foxp3 mRNA expression is indicated by circle. Student's t-test was used to calculate significance ($p<0.05$, false discovery rate adjustment of 0.3, and 1.5x differential expression), and revealed 1.68% differential gene expression on the 430a 2.0 Affymetrix chip (right panel). Data are shown after z-score transformation. Hierarchical clustering was calculated using Rapid Neighbor Joining with Euclidean distance measure.

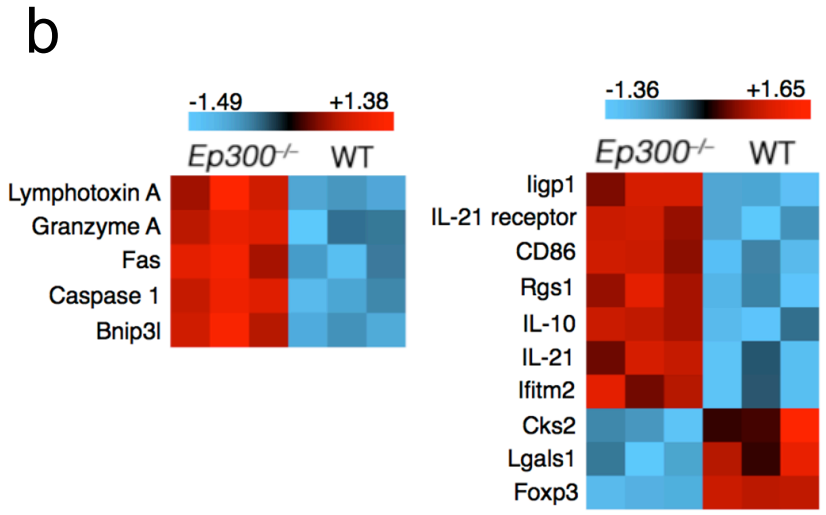

Fig. S2b: Loss of *Ep300* in Foxp3+ T_{regs} leads to upregulation of pro-apoptotic genes and downregulation of multiple genes important to normal Treg biology. Microarray showing differential expression of pro-apoptotic genes (left panel) and biologically important Treg genes (right panel) between WT and *Ep300*$^{-/-}$ Tregs. Data were z-score transformed for display. Abbreviations: Fas, Fas receptor (CD95); Bnip3l, BCL2/adenovirus E1B 19 kDa protein-interacting protein 3-like; ligp1, Interferon inducible GTPase 1; Rgs1, Regulator of G-protein signaling 1; Ifitm2, Interferon induced transmembrane protein 2; Cks2, CDC28 protein kinase regulatory subunit 2; Lgas1, Lectin, galactose binding, soluble 1.

Supplementary Figure 3: Cellular effects of *Ep300* deletion

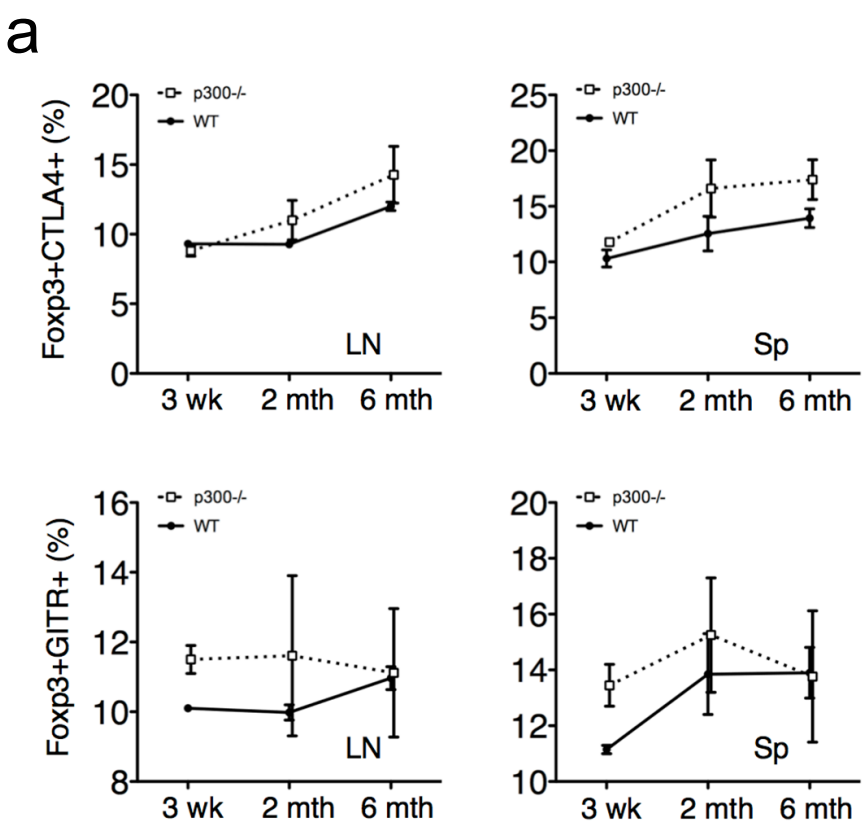

Fig. S3a: Deletion of p300 in Tregs did not affect their expression of CTLA4 or GITR within lymph nodes (LN) or spleen (Sp). Cells were gated on the CD4⁺ cells. Data representative of 2 experiments, each involving 4 mice/group/time-point.

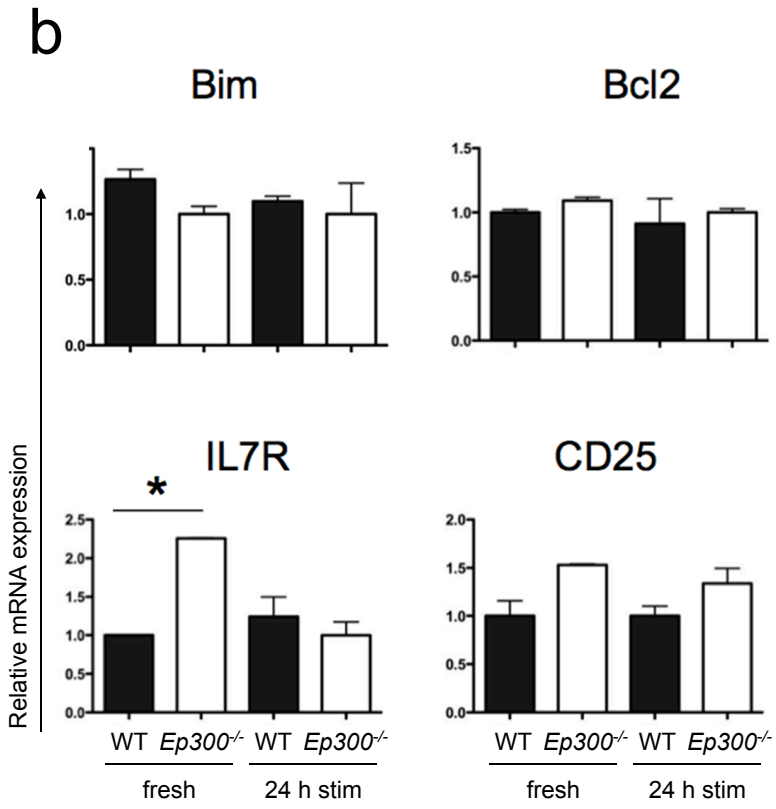

Fig. S3b: qPCR analyses of indicated gene expression in CD4+YFP+ Tregs from WT or *Ep300*$^{-/-}$ mice. High purity Tregs were untreated or treated with CD3/CD28 mAbs for 20 h in vitro. qPCR data were normalized to 18S (*p<0.05), and data (mean ± SD) are representative of 2 independent experiments involving 4 mice/group.

Supplementary Figure 4: Foxp3 dependent deletion of *Ep300* impairs T_{reg} suppressive function in vitro

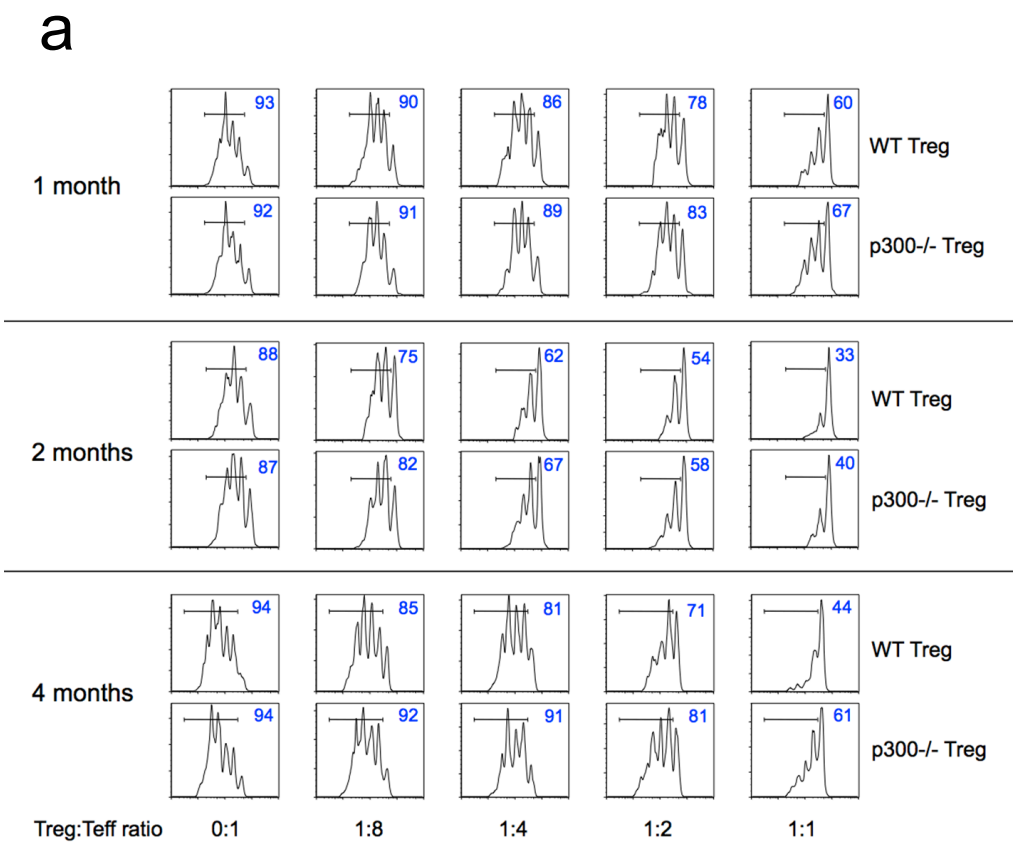

Fig. S4a: Treg deletion of *Ep300* impairs T_{reg} suppressive function in vitro. CFSE-labeled $CD4^+CD25^-$ T cells were incubated with the indicated ratios T_{reg} cells isolated from 1, 2 or 4 month old *Ep300*$^{-/-}$ and WT mice, in the presence of irradiated APC and CD3 mAb. The percentage of proliferating T_{eff} cells is shown in each panel; data are representative of 3 such assays.

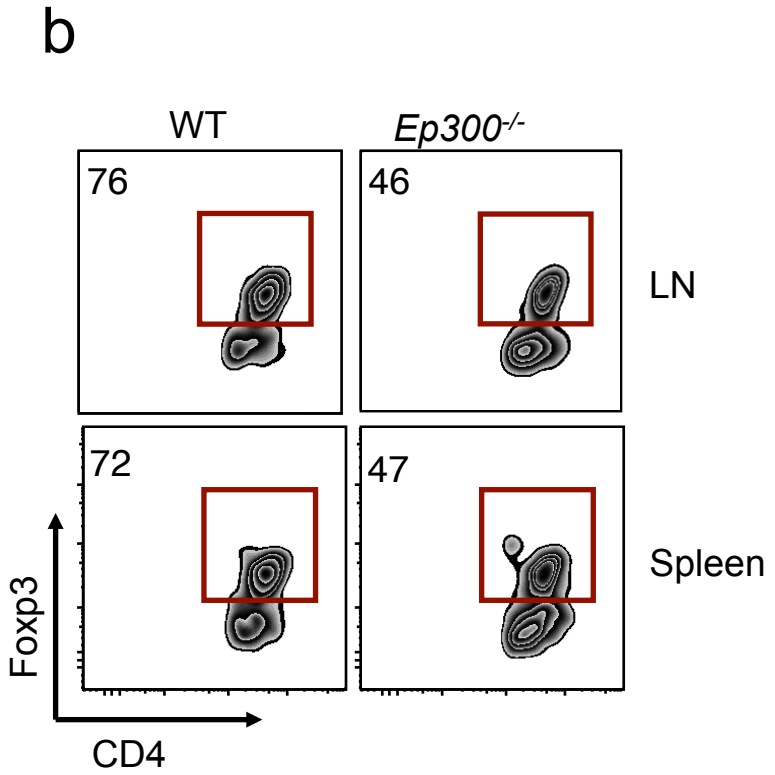

Fig. S4b: Decreased proportions of *Ep300*$^{-/-}$ vs. WT Tregs in lymphoid tissues of Rag1$^{-/-}$ mice 7 days post-adoptive transfer. Numbers in quadrants indicate the percentage of CD4+Foxp3+ cells. 1 × 10^6 $Thy1.1^+CD4^+CD25^-$ T_{eff} and 5 × 10^5 *Ep300*$^{-/-}$ vs. WT T_{regs} were adoptively transferred to Rag1$^{-/-}$ mice. 7 days later, lymph nodes and spleens were harvested and subjected to flow cytometric analysis. Data are representative of 2 experiments.

Supplementary Figure 5

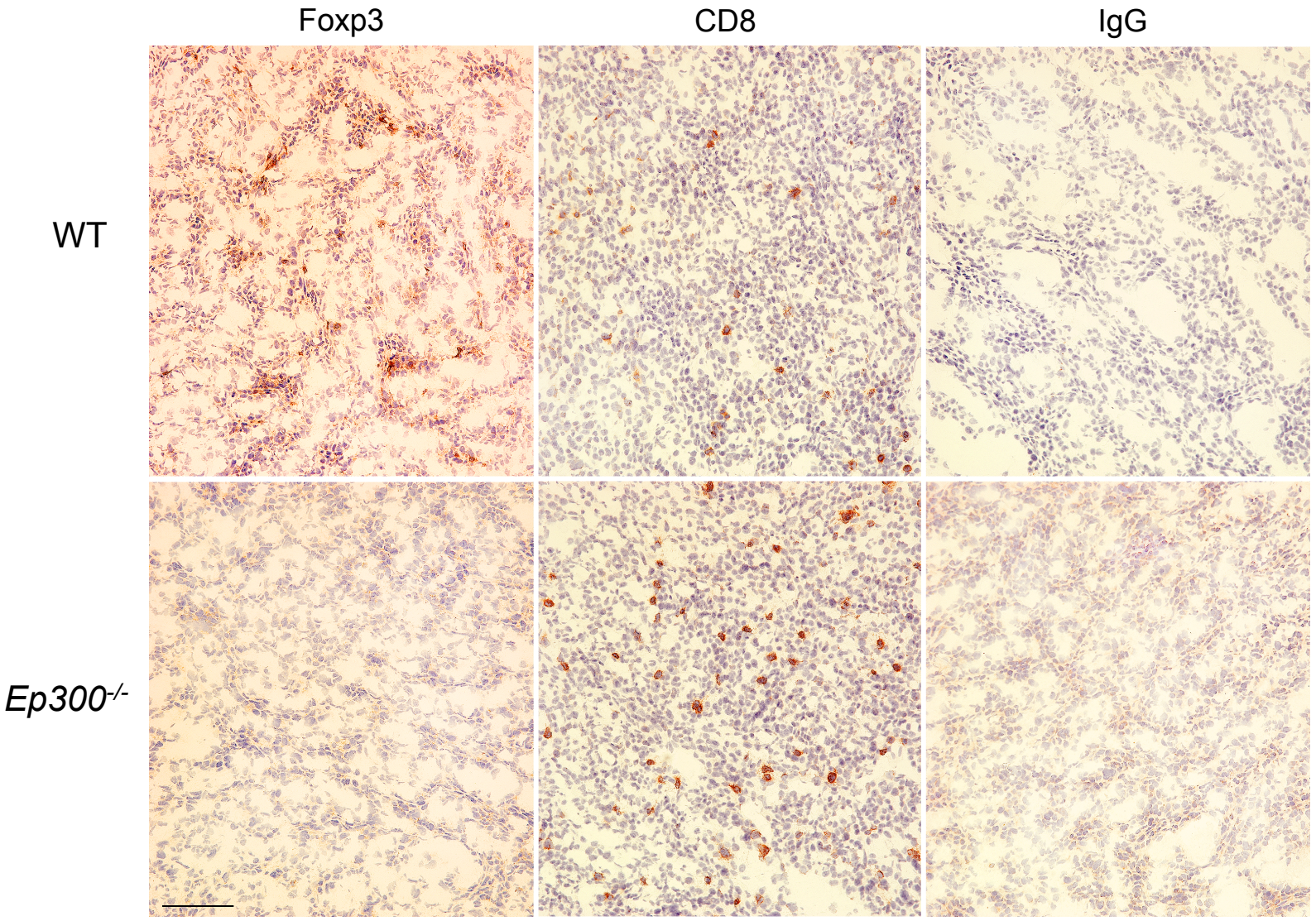

Fig. S5: *Ep300* deletion markedly decreased intratumoral Foxp3$^+$ cells and increased infiltration by CD8$^+$ T-cells. TC1 tumors in immunocompetent C57BL/6 mice were harvested at day 18; hematoxylin counterstain, and scale bar indicates 100 μm.

Supplementary Figure 6: Use of p300i impairs Foxp3$^+$ T_{reg} function in vitro and in vivo

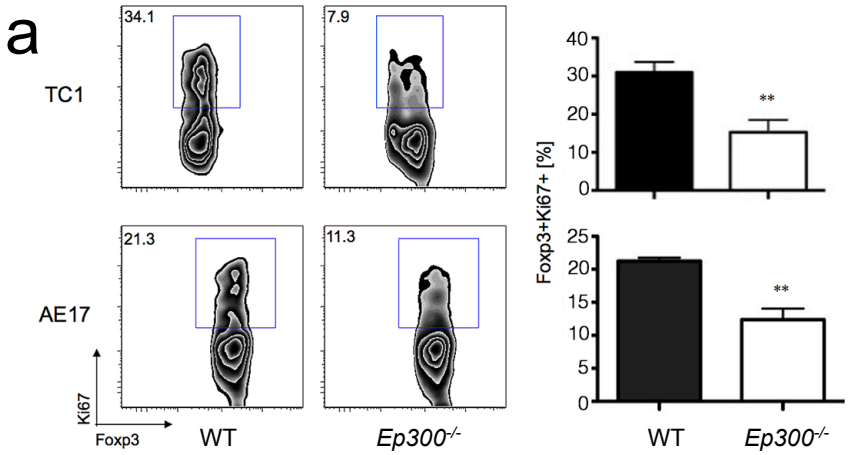

Fig. S6a: Decreased proportions of Foxp3+Ki67+ cells in spleens of *Ep300*$^{-/-}$ vs. WT tumor-bearing mice; TC1 (upper) and AE.17 (lower). Splenocytes from tumor-bearing mice were stained for CD4, Foxp3 and Ki67, and analyzed by flow cytometry, with gating on CD4$^+$ cells; percentages of labeled cells are shown in each quadrant; 6-7 mice/group and ** indicates p<0.01.

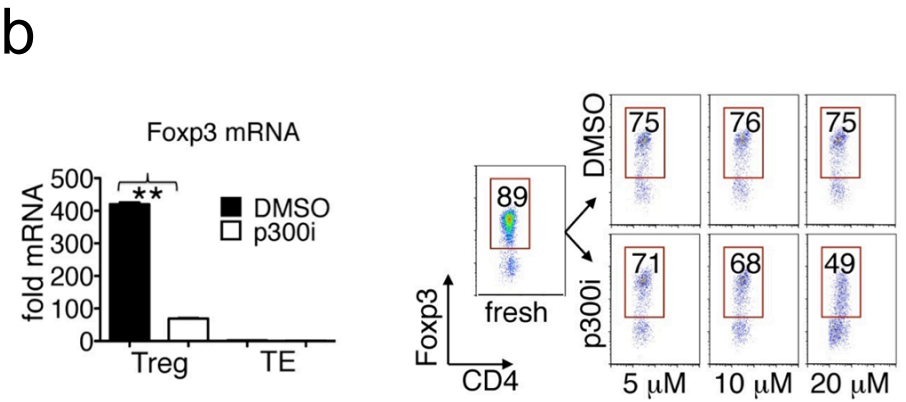

Fig. S6b: Use of p300i in vitro decreased T_{reg} mRNA and protein levels. Left panel shows T_{reg} isolated from 10 wk old B6 mice were treated with DMSO or p300i for 20 h. mRNA was extracted for qPCR analysis, with normalization to 18s (**p<0.01). In addition, p300i impaired CD4$^+$Foxp3$^+$ expression at the indicated concentrations (right panel); data are representative of 3 independent experiments, with 4 mice/group.

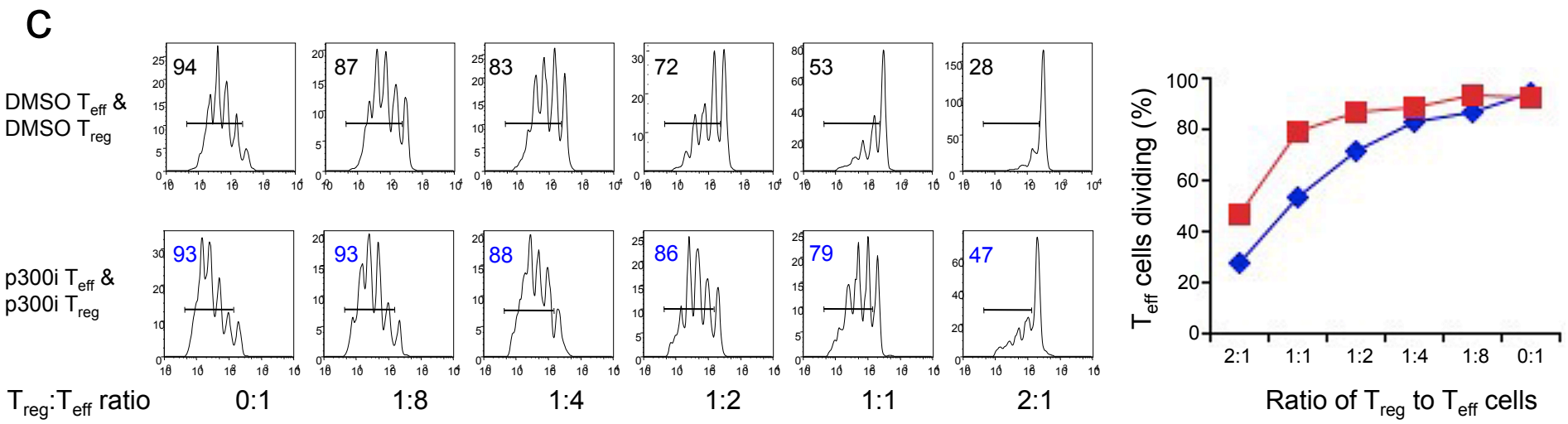

Fig. S6c: Use of p300i *in vivo* decreased T_{reg} suppressive function. C57BL/6 mice received DMSO or p300i (8.9 mg kg^{-1} d^{-1}, i.p.) for 1 week, followed by isolation of T_{reg} and T_{eff} cells. *In vitro* T_{reg} suppression assays were performed using 5 × 10^5 CFSE-labeled T_{eff} cells stimulated with CD3 mAb in the presence of an equal number of irradiated APC, plus the indicated ratios of T_{reg} cells. Data was summarized in the panel at right, in which the red line indicates p300i treated mice, and the blue line indicates DMSO treated mice. Data are representative of 3 independent experiments involving 4 mice/group.

Supplementary Figure 7: Use of p300i does not affect proportions of T-cell subsets

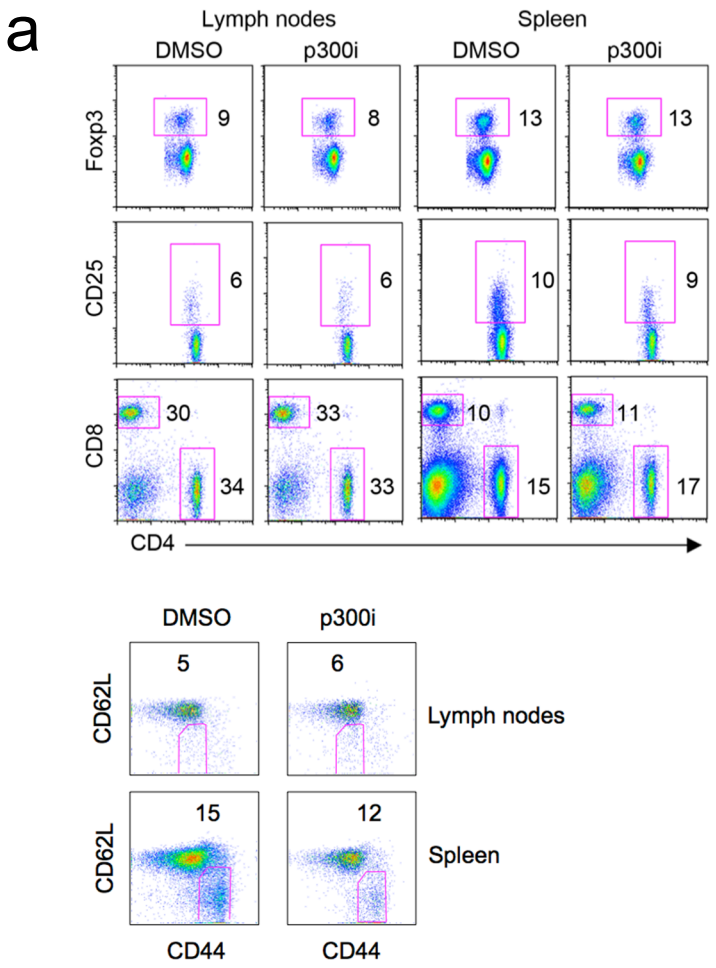

Fig. S7a: Use of p300i *in vivo* did not affect key T-cell subsets. Flow cytometric analysis of T-cell subsets after 1 week of in vivo treatment with p300i (8.9 mg kg^{-1} d^{-1}) or DMSO control. Percentages of CD4, CD8, CD25 (upper panel), and $CD44^{high}$ and $CD62L^{low}$ cells (lower panel) are shown; data are representative of 3 independent experiments.

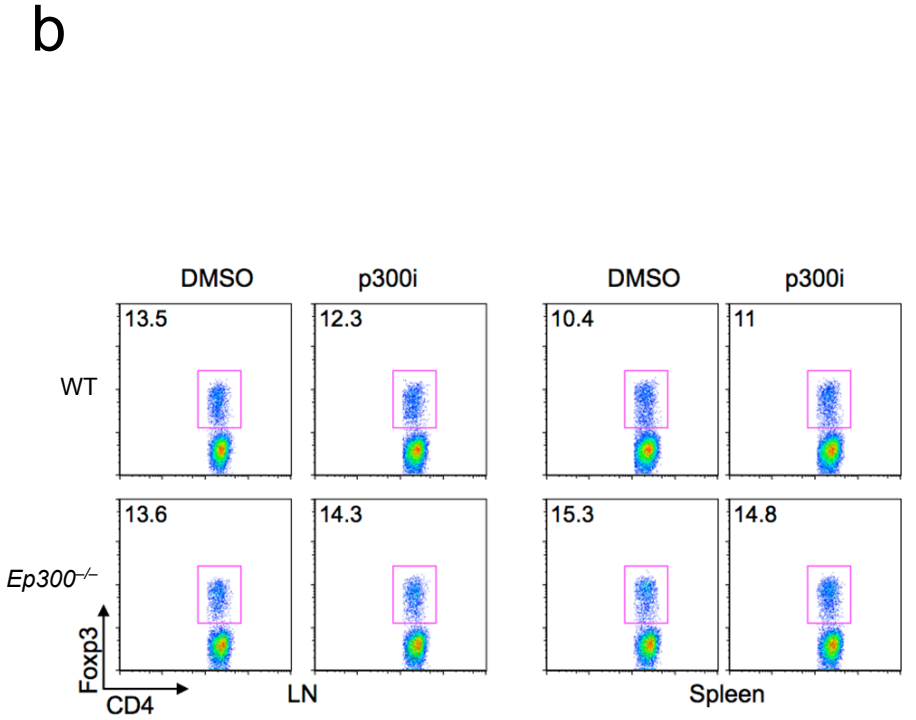

Fig. S7b: p300i in vivo treatment did not affect proportions of Foxp3+ T_{reg} in the lymph nodes and spleens of WT or *Ep300*$^{-/-}$ mice. Flow cytometric analysis of percentages of CD4+Foxp3+ cells after 1 week of in vivo treatment with p300i (8.9 mg kg^{-1} d^{-1}) or DMSO control (delivered by pump) in WT or *Ep300*$^{-/-}$ mice. 3 mice/ group.

Supplementary Figure 8: Use of p300i does not affect T_{eff} alloreactivity in vivo

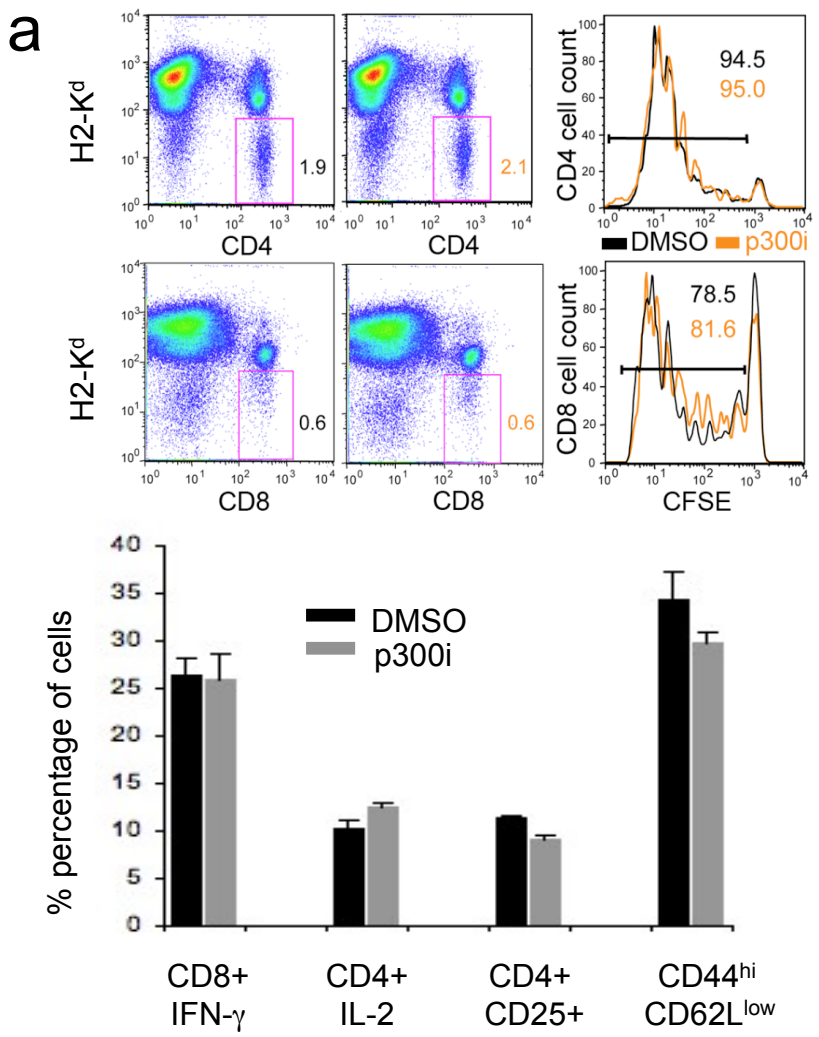

Fig. S8a: Parent-to-F1 assay in which CFSE-labeled T-cells from C57BL/6 mice were injected into B6D2F1 mice (n=3) and recipients were treated i.p. with p300i (8.9 mg kg^{-1} d^{-1}) or DMSO for 3 d. After 3 d, donor cells (H2-K^d negative) were analyzed by flow cytometry for alloantigen-induced cell activation and proliferation (upper panel), and for intracellular cytokine production (lower panel); none of the data in panels a and b were significantly different when using p300i versus DMSO alone (p>0.05). Data are representative of 2 independent experiments, with 4 mice/group.

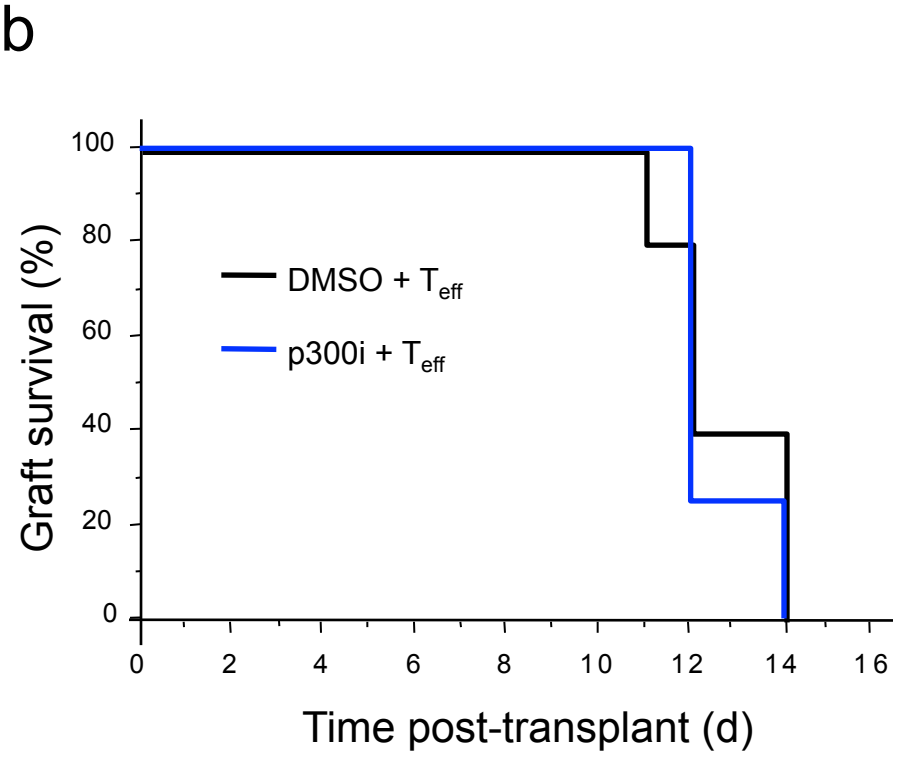

Fig. S8b: Use of p300i *in vivo* did not affect T cell-mediated acute cardiac allograft rejection. B6/RAG1-/- mice (n=4/group) were engrafted with fully MHC-mismatched BALB/c cardiac allografts, and were adoptively transferred with 1×10^6 C57BL/6 mice $CD4^+CD25^-$ conventional T-cells. Alzet pumps were used to deliver p300i (8.9 mg/kg/d) or DMSO.

Supplementary Table 1

Histopathology of male mice (10 weeks of age) with conditional deletion of *Ep300* in T_{regs}[1]

Tissue	Histologic findings
Bone marrow	Normocellular marrow with tri-lineage hematopoiesis and a myeloid to erythroid ratio of 3:1.
Lung	Lungs demonstrate patchy, mild perivascular and peribronchiolar lymphocytic inflammation. Infiltrates are primarily centered on large bronchovascular bundles and extend to involve distal airspaces, with minimal widening of intra-alveolar septae.
Liver	Overall architecture is intact with mild to moderately dense lymphocytic infiltration involving the majority of large and small portal tracts. Inflammation is also seen within the lobules, and there is diffuse extramedullary hematopoiesis characterized by scattered collections of erythroid precursors and occasional megakaryocytes within sinusoids.
Spleen	Splenic parenchyma is normal with well-organized peri-arteriolar lymphoid sheaths and lymphoid follicles. Scattered foci of extramedullary hematopoiesis are identified within the intact red pulp.
Lymph nodes	Nodes display normal cellularity but there is effacement of nodal architecture, with loss of distinct follicles; germinal center formation is inconspicuous.
Thymus	Overall thymic architecture is intact with preservation of distinct corticoid-medullary junctions. No apparent decrease in the volume of cortical thymocytes is identified.
Skin	A diffuse, mildly cellular mononuclear inflammatory infiltrate predominantly composed of small mature lymphocytes is present within the superficial dermis with focal exocytosis.
Brain	The brain is normally developed without significant leptomeningeal or parenchymal inflammation.
Pancreas	Pancreata are normally developed with well-formed islets of Langerhans. Rarely, perivascular inflammation is noted in peri-pancreatic adipose tissue.
Heart	Unremarkable cardiac myocytes; rare foci of extramedullary hematopoiesis.
Kidney	Renal parenchyma, including glomeruli and tubules, is normally developed. No significant interstitial or perivascular inflammation is seen.
Gastro-intestinal tract	The small bowel contains scattered collections of mononuclear cells in the lamina propria without infiltration into surface epithelium. Villous architecture is intact.

[1] Tissues from 4 mice/group for histologic were fixed in 10% neutral buffered formalin, routinely processed, embedded in paraffin and stained with hematoxylin and eosin; comments are for mice with deletion of p300 within T_{regs} as compared to features in littermate and WT controls.

Supplementary Table 2

Autoantibody screening of sera from male mice with conditional deletion of *Ep300* in T_{regs}[1]

Type of autoantibodies	Presence at 3-4 weeks of age	Presence at 10-12 weeks of age	Substrate
Anti-nuclear	No	No	Liver, kidney, pancreas and other tissues
Anti-mitochondrial	No	No	Liver, kidney, stomach
Anti-smooth muscle	No	No	Small & large intestines, stomach
Anti-striated muscle	No	No	Striated muscle
Anti-endomysium	No	Yes, titer of 1/20-1/40, in 20% of mice	Striated muscle
Anti-islet cell	No	Yes, titer of 1/5-1/10 in 20% of mice	Pancreas, islets
Anti-steroid hormone-producing cells	No	No	Adrenal gland, ovaries, testis
Anti-thyroid peroxidase	No	No	Thyroid gland, cytoplasm of the follicle epithelium
Anti-keratin antibodies	No	No	Ear, stratified squamous keratinizing epithelium
Anti-parietal cell	No	Yes, titer of 1/20-1/40, in 20% of mice	Stomach

[1]Indirect immunofluorescent staining of cryostat sections of tissues from healthy mice, using sera (diluted 1:5) from WT or p300-/- mice.